

# Comparative x-ray and dielectric measurements of smectic *A*–smectic-*C*\* transition in bulk and confined geometries

K. L. Sandhya,<sup>1</sup> S. Krishna Prasad,<sup>1</sup> D. S. Shankar Rao,<sup>1</sup> and Ch. Bahr<sup>2</sup>

<sup>1</sup>Centre for Liquid Crystal Research, Jalahalli, Bangalore 560 013, India

<sup>2</sup>Institute of Physical Chemistry, University of Marburg, D-35032 Marburg, Germany

(Received 1 May 2002; published 24 September 2002)

Comparative x-ray and dielectric measurements have been made on a liquid crystal exhibiting a smectic-*A*–chiral-smectic-*C* (smectic-*C*\*) transition in bulk and confined geometries. It is observed that confining the material in Anopore membranes having 200-nm pore size leads to the following features: (1) the temperature dependence of the x-ray layer spacing shows a qualitatively different behavior, (2) in the smectic-*A* phase the soft mode relaxation frequency increases by a factor of 2.5, and (3) in the smectic-*C*\* phase the relaxation frequency of the Goldstone mode increases dramatically by as much as 400 times, perhaps owing to a partial unwinding of the helix by the surface induced field.

DOI: 10.1103/PhysRevE.66.031710

PACS number(s): 61.30.–v, 64.70.Md

## I. INTRODUCTION

It is known that the behavior of liquid crystalline transitions can be strongly influenced by geometrical restrictions [1]. Various types of porous materials have been used to confine or impose geometrical restrictions on the liquid crystalline materials. They are (i) polymer matrices (polymer dispersed liquid crystals) having well-defined spherical or ellipsoidal cavities, (ii) porous glasses with narrow pore size distributions but randomly oriented and interconnected pores, (iii) silica gels and aerosil with broad pore size distributions and irregular shapes of the cavities, and (iv) porous filters such as Millipore, Nucleopore, and Anopore membranes. Of these, the Anopore membranes are attractive as they have highly parallel cylindrical pores with narrow size distributions and smoother cavity surface. Most of the work reported in this field has been devoted to the isotropic–nematic transition (iso-*N*) [2–6], although transitions involving smectic-*A* (Sm-*A*) [7,8], chiral smectic-*C* (Sm-*C*\*) [9–11], and crystal-*B* [12,13] phases have also been studied. An important influence of confinement is that it affects the nature of the transition. In the case of the Iso-*N* transition, for example, a weakening of the first-order character and also a broadening of the two-phase region associated with the transition have been observed. In fact, for sufficiently small pore diameters, the high temperature phase is not truly isotropic as a small residual orientational order persists well above the transition; in such a case the isotropic phase is referred to as the paranematic phase. These effects can be so strong that the Iso-*N* transition could be completely absent and a gradual increase of the local orientational order is seen as the temperature is lowered. Another, but related, feature observed is the depression in the transition temperature when the material is confined in a porous media. Suppression of thermal fluctuation in the nematic order parameter has also been presented as a reason for some of the effects observed in confined geometry studies [1]. In this paper, we present the results of differential scanning calorimetry (DSC), x-ray diffraction, and dielectric studies on a compound exhibiting Sm-*A*–Sm-*C*\* transition, in bulk and also in confined geometries.

## II. EXPERIMENTAL

Measurements have been carried out on 4-(3-methyl-2-chlorobutanoyloxy)-4'-heptyloxy biphenyl (*A7* for short), having the following phase sequence in bulk [14] Iso(81.7 °C) Sm-*A*(73.1 °C) Sm-*C*\*(71.1 °C) Cr-*G*(63.3 °C) Cr-*H*. Here Cr-*G* and Cr-*H* stand for the three-dimensionally ordered crystal-*G* and *H* phases, respectively, considered earlier as smectic-*G* and smectic-*H* phases. For measurements in confined geometry, the sample was filled in Anopore membranes (Whatman, USA). These membranes are made from aluminum oxide and have parallel cylindrical pores penetrating the 60 μm thickness normally, with a nominal pore size of 200 nm. The membranes were treated with a long chain acid (palmitic acid), a treatment known to induce alignment of the molecules in the plane of the membrane [1]. The procedure adapted to fill the sample into the pores of the Anopore membrane is described elsewhere [13]. Calorimetry experiments were done using a Perkin Elmer DSC7. For measurements on a bulk sample, an empty cup was used as a reference; for measurements on Anopore membranes an unfilled membrane of approximately the same size was placed in the reference cup. X-ray experiments were done with the help of an (MAC Science DIP1030) image plate setup. For dielectric experiments on bulk samples, the material was sandwiched between two indium tin oxide (ITO)-coated glass plates with a polyimide layer for promoting planar orientation of the molecules. For measurements on Anopore sample the membrane containing the sample was sandwiched between two ITO-coated glass plates serving as electrodes. A wide-frequency range impedance analyzer (Sotatron model 1260) along with a broadband dielectric converter (BDC-N, Novocontrol), and controlled by WINDETA software (Novocontrol) was used to carry out the dielectric experiments.

## III. RESULTS AND DISCUSSION

### A. DSC measurements

Figure 1 shows DSC scans obtained with the bulk and Anopore samples while cooling the sample at a rate of

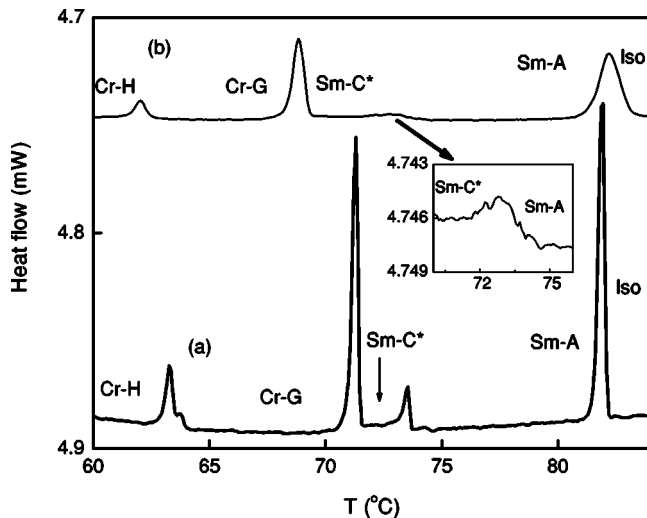


FIG. 1. Differential scanning calorimetric scan in the cooling mode for (a) the bulk and (b) the Anopore sample. It should be noted that for all the transitions the peak width is more and the peak height is lower for the Anopore sample than for the bulk sample. Inset shows on an enlarged scale the scan in the vicinity of the Sm-A–Sm-C\* transition for the Anopore sample. (Cooling rate 5 °C/min.)

5 °C/min. It must be mentioned here that the Anopore membrane used for these experiments was a small piece cut from a full membrane filled with the sample. This, in addition to the fact that the data for the density of the pores given by the manufacturer are only correct to an order of magnitude, prevented an accurate determination of the amount of sample in the membrane. For this reason we have normalized the scans by dividing the two sets of data by the corresponding heat of transition for the isotropic-smectic-A transition. The four peaks seen for the bulk sample (profile *a* in Fig. 1) correspond to the Iso-Sm-A, Sm-A–Sm-C\*, Sm-C\*–Cr-G and Cr-G–Cr-H transitions. This phase sequence and the associated transition temperatures are in agreement with the data reported in the literature. The scan for the Anopore sample looks qualitatively similar, and therefore we presume that it has the same phase sequence as that of the bulk sample (profile *b* in Fig. 1). X-ray studies, to be discussed later, corroborate this argument. The confinement of the sample in the membrane, however, introduces some differences. First, it broadens the transitions, by a factor of 3.6, 6.7, 1.8, and 1.4 times for Iso-Sm-A, Sm-A–Sm-C\*, Sm-C\*–Cr-G, and Cr-G–Cr-H transitions, respectively. Second, the peak height is reduced and rounded for all the transitions, especially so for the Sm-A–Sm-C\* transition with one order of magnitude reduction in the peak height (see inset of Fig. 1). In fact, the signal due to this transition becomes quite weak and difficult to locate with slower cooling rates. We also observe confinement-induced shift in the transition temperatures. While the Iso-Sm-A transition shows a small (0.2 °C) upward shift, the temperatures for the other transitions are lower in the Anopore sample. The largest shift seen is for the Sm-C\*–Cr-G transition with a temperature 2.5 °C; this results in an increase in the temperature range of the Sm-C\* phase from 2.2 °C in the bulk to 4 °C in the Anopore sample.

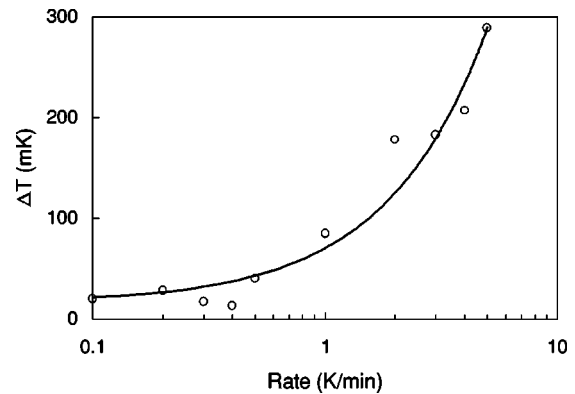


FIG. 2. Plot of thermal hysteresis,  $\Delta T$  defined as the difference in Sm-A–Sm-C\* transition temperature between the heating and cooling scans as a function of heating/cooling rate for the bulk sample. Note that the horizontal scale is logarithmic. On a linear scale the solid line would represent a linear function.

It may be recalled that transition shifts, peak height suppression, and broadening of the transition upon confinement in narrow pores has been well documented in the literature. As an example of the features seen at the Iso-Sm-A transition, we quote the case of decyl cyano biphenyl (10CB) when the sample is confined in Anopore membranes treated to obtain radial alignment of the molecules. Specific heat data of Iannacchione and Finotello [4] demonstrated that the Iso-Sm-A transition shows all the features mentioned above for our sample. In particular, both the samples show an upward shift in  $T_{Iso-Sm-A}$  upon confinement, the values being not very different (0.08 °C for 10CB and 0.26 °C for our sample A7). Now we discuss the results for the Sm-A–Sm-C\* transition, our prime interest in this paper. It has been proved by x-ray and specific heat measurements [15,16] that the Sm-A–Sm-C\* transition in this material has a first-order character, albeit weakly so. In the following, we show that DSC measurements are sensitive enough to demonstrate this feature. An important characteristic of a first-order transition is the presence of temperature hysteresis; there is a finite difference ( $\Delta T$ ) between the transition temperatures obtained in the heating and cooling modes. Figure 2 shows a plot of  $\Delta T$  versus the heating/cooling rate for the bulk sample. The data that can be described by a linear fit yield a value of  $\Delta T = 15$  mK at zero heating/cooling rate. Surprisingly, this value is in close agreement with the value of 18 mK obtained using a state-of-the-art ac calorimeter [16]. The smallness of this value suggests that although the transition is first order, it is an extremely weak one. As mentioned earlier, confining the sample in Anopore broadens the transition. Therefore, the absence of thermal signature associated with the Sm-A–Sm-C\* transition at lower heating/cooling rates in Anopore membranes could be either because the transition has become second order or the broadening makes the signal too weak to be detected.

## B. X-ray measurements

Figures 3(a) and 3(b) show intensity versus  $2\theta$  profiles extracted from the x-ray-diffraction patterns obtained in the

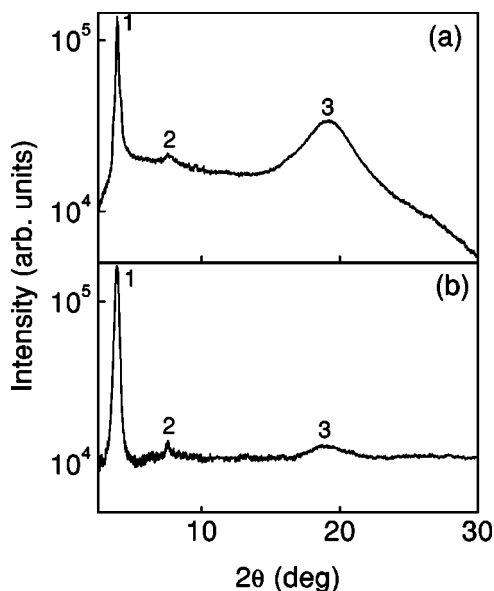


FIG. 3. One-dimensional x-ray intensity vs  $2\theta$  profile in the Sm-A phase of the bulk [Fig. 3(a)] and Anopore [Fig. 3(b)] samples. Two sharp reflections at low angles (numbered 1 and 2) correspond to first- and second-order diffractions from the smectic layer structure. The broad diffuse peak at wide angles  $\sim 20^\circ$  corresponds to a liquidlike order within the smectic layers.

Sm-A phase of both the bulk and Anopore samples. Both the profiles show two sharp (one very strong and another weak) reflections at low angles. The layer spacing ( $d$ ) for the weak one is half of that for the strong one. They correspond to the first- and second-order diffractions from the smectic layer structure. The  $d/L$  ratio ( $L$  being the length of the molecule in its most extended form) is 0.96 expected for the monomolecular Sm-A layer structure known for this material. The  $d/L$  ratio being  $< 1$  is due to the well-known fact that the alkyl chains are in the molten form. However, notice that the  $d$  value (and consequently the  $d/L$  ratio) is slightly larger for the Anopore sample than for the bulk. This is perhaps due to a slight stretching of the alkyl chains caused by the suppression of thermal fluctuation in the confined geometry. In addition to the two low angle reflections a broad diffuse peak is seen at wide angles, centered at  $2\theta \sim 20^\circ$ , typical of the scattering from correlations between molecules within individual layers. The diffractograms in the Sm- $C^*$  phase were qualitatively similar to the ones in the Sm-A phase, although the diameter of the low angle reflections were larger and varying with temperature, due to the tilt of the molecules with respect to the layer normal. The temperature variation of the layer spacing in the bulk and Anopore samples is shown in Fig. 4(a) and 4(b), respectively. For the bulk sample there is an abrupt decrease in spacing across the Sm-A–Sm- $C^*$  transition. However, no two-phase region with coexistence of peaks due to both the Sm-A and Sm- $C^*$  phases was observed. It may be noted that such a coexistence is characteristic of a first-order transition and was indeed reported earlier [15] for the compound studied here. But the resolution of our present setup is not sufficient to separate out the individual contributions of the Sm-A and Sm- $C^*$  phases in the two-

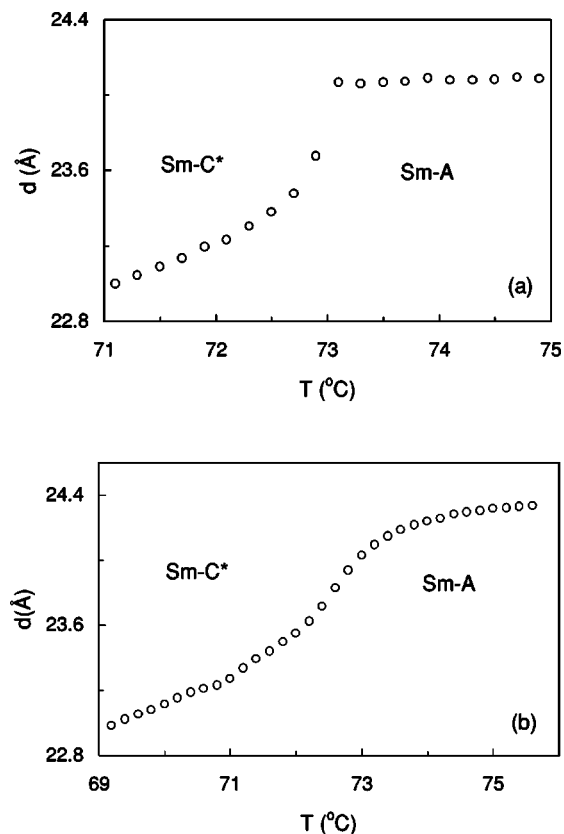


FIG. 4. Thermal variation of the layer spacing for the bulk [Fig. 4(a)] and for the Anopore [Fig. 4(b)] samples near the Sm-A–Sm- $C^*$  transition. While the Anopore sample shows a smooth variation, the bulk sample exhibits an abrupt change across the transition.

phase region. In contrast, the Anopore sample showed a smooth variation in layer spacing across the Sm-A–Sm- $C^*$  transition. The tilt angle in the Sm- $C^*$  phase has been calculated by assuming the rigid rod model according to which  $\theta = \cos^{-1}(d_{Sm-C^*}/d_{Sm-A})$ . For this purpose, the value of  $d_{Sm-A}$  was taken to be the one at the transition. The thermal variation of  $\theta$  thus calculated for the bulk and Anopore samples are shown in Fig. 5. As mentioned earlier, the resolution of our setup is not sufficient to separate out the individual contributions of the Sm-A and Sm- $C^*$  phases in the two-phase region. Therefore for the bulk sample a jump in  $\theta$ , which is the order parameter for the Sm- $C^*$  phase, is not seen, rather a steep variation at the transition is observed. In contrast, the Anopore sample shows a much smoother variation in  $\theta$  as the temperature is decreased into the Sm- $C^*$  phase. In the light of the DSC measurements mentioned earlier, we have attempted to describe the temperature variation of tilt angle in terms of an extended mean field proposed by Huang and Viner [17]. According to this model a generalized way of describing the order parameter variation near a Sm-A–Sm- $C^*$  transition is to write the free energy of the system as

$$F = F_o + \frac{1}{2}a\theta^2 + \frac{1}{4}b\theta^4 + \frac{1}{6}c\theta^6.$$

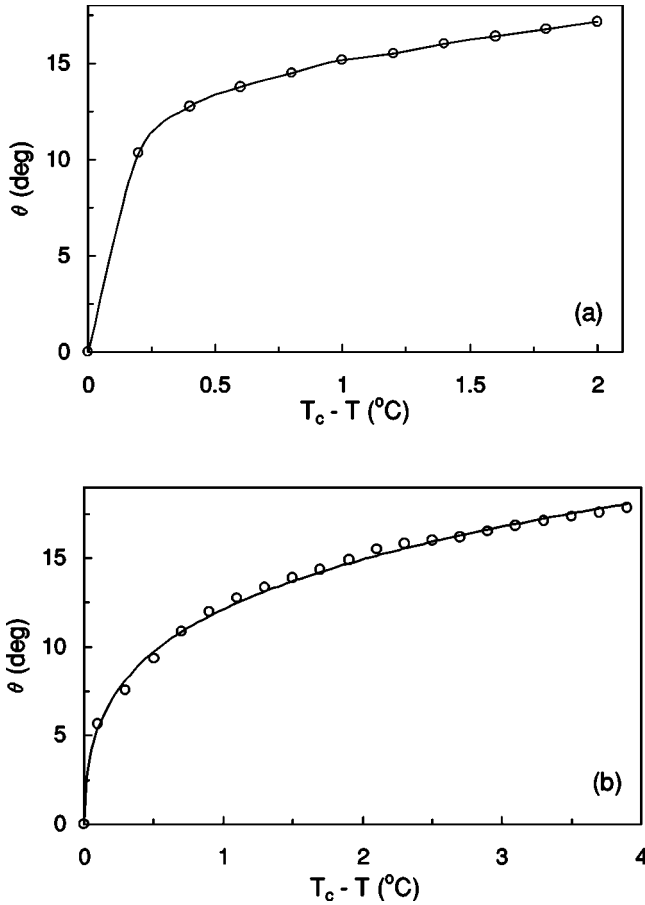


FIG. 5. Temperature variation of the tilt angle  $\theta$  in the Sm- $C^*$  phase for the bulk [Fig. 5(a)] and Anopore samples [Fig. 5(b)]. Whereas the solid line in Fig. 5(b) represents a fit to an extended mean-field model [Eq. (1)], it acts as only a guide to the eye in Fig. 5(a).

Here  $a = a_0 t$ , with  $t = (T - T_c)/T_c$ , and  $b$  and  $c$  are temperature-independent coefficients. Minimizing this expression gives two solutions for  $\theta$ ,

$$\theta = 0, \quad (1)$$

$$\theta = \left[ R \left( 1 + \frac{3t}{t_0} \right)^{1/2} - 1 \right]^{1/2},$$

where  $R = b/3c$ . In this model  $t_0$  is an all important parameter, describing the crossover temperature at which the behavior changes from mean-field-like to tricritical-like; the nearer the value is to zero, closer it is to the tricritical point. As the bulk sample is known to have an extremely weak first-order transition we do not fit the bulk data to Eq. (1). (An attempt to do so will lead to very small values of  $t_0$ , apparently indicating that the system lies very close to a tricritical point). In contrast, the smoother variation of  $\theta$  with temperature for the Anopore sample, makes it a better candidate to perform such a fitting, which is shown in Fig. 5. The values of  $t_0$  obtained is  $0.0024 \pm 0.001$ , which suggests that the transition is a second-order one and quite far away from a tricritical point. An equally possible explanation is the

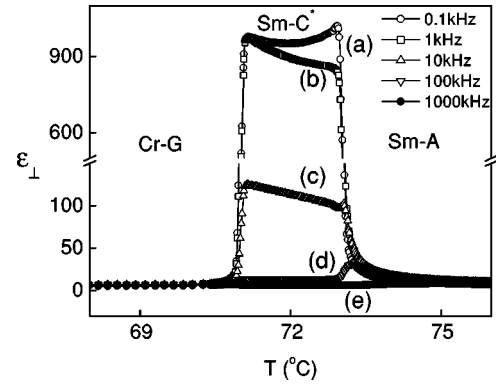


FIG. 6. Temperature variation of the static dielectric constant perpendicular to the director ( $\epsilon_{\perp}$ ) at different frequencies for the bulk sample. The curves marked (a)–(e) stand for data measured with 0.1 kHz, 1 kHz, 10 kHz, 100 kHz, and 1000 kHz, respectively. The sharp increase and the precipitous drop seen at low frequencies for the Sm- $A$ –Sm- $C^*$  and Sm- $C^*$ –Cr- $G$  transitions are as expected. Notice that  $\epsilon_{\perp}$  decreases with increasing frequency, particularly in the Sm- $C^*$  phase. The large change between 1 kHz and 10 kHz in the Sm- $C^*$  phase indicates the frequency range of the Goldstone mode relaxation.

following. It has been observed that application of an electric field drives the first-order Sm- $A$ –Sm- $C^*$  transition towards a critical point. In such a situation there would be also a finite tilt angle in the Sm- $A$  phase [18], and therefore the temperature dependence of the layer spacing would not look very different from the one shown Fig. 4(b). It is possible that a surface field, arising out of the interactions of the liquid crystalline molecules with the Anopore membrane, mimics the role played by the electric field in the case mentioned above, leading to a continuous evolution of the layer spacing.

### C. Dielectric measurements

Figure 6 shows the temperature variation of the sample dielectric constant perpendicular to the director ( $\epsilon_{\perp}$ ) at different fixed frequencies for the bulk sample. These measure-

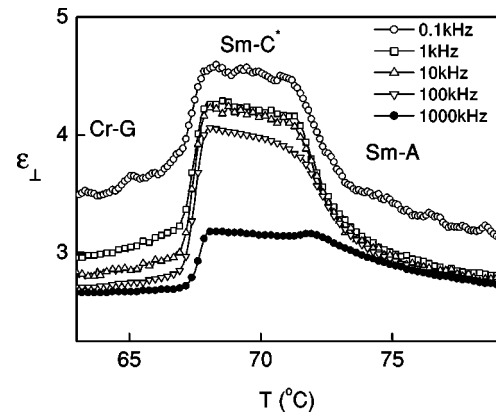


FIG. 7. Thermal variation of  $\epsilon_{\perp}$  at different frequencies for the Anopore sample. Notice that the overall behavior is qualitatively similar to that for the bulk sample. However, the smaller value for the  $\epsilon_{\perp}$  for the Anopore sample compared to that for the bulk sample could be due to the partial suppression of the Goldstone mode.

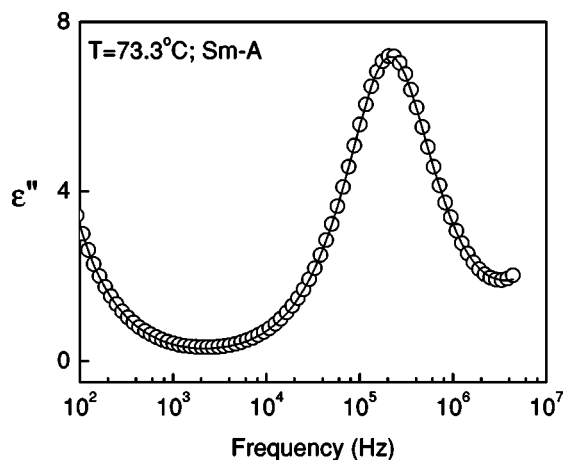


FIG. 8. Plot of  $\epsilon''$  vs frequency (loss curve) for the bulk sample in the Sm-A phase. Solid line is a fit to the Havriliak-Negami function [19] along with the conductivity term (see text). The behavior at low frequency is due to the presence of ionic impurities in the sample.

ments were done using a 40- $\mu\text{m}$ -thick ITO-coated glass cell with the substrate surfaces treated for planar alignment of the molecules. For the measuring frequency of 0.1 and 1 kHz, the onset of the Sm-A–Sm- $C^*$  transition is marked by a large increase in the  $\epsilon_{\perp}$  value. The large magnitude of  $\epsilon_{\perp}$  in the Sm- $C^*$  phase is expected for a compound with high spontaneous polarization. When the frequency is increased, although the qualitative behavior remains the same, there is a substantial decrease in the value. With a further increase in frequency to 100 kHz, the behavior also changes, having a peaklike appearance at the transition. The features seen in the Sm- $C^*$  phase at low frequencies suggest the presence of a significantly active Goldstone mode having a relaxation frequency in the range of 1–10 kHz. The peaking of the data at 100 kHz is indicative of the soft mode arising out of tilt fluctuations. Across the Sm- $C^*$ –Cr-G transition,  $\epsilon_{\perp}$  drops to quite low values even at low frequencies. The results for the Anopore sample are shown in Fig. 7. The most significant

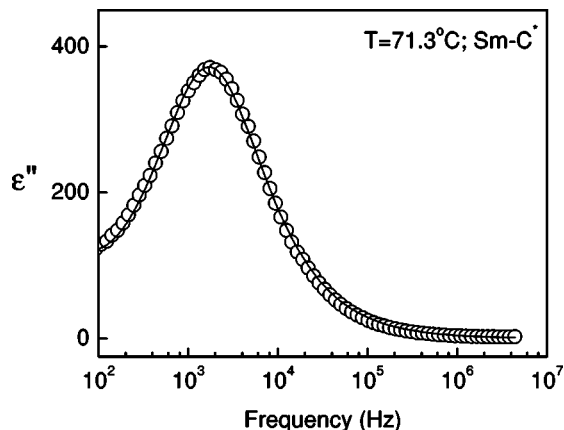


FIG. 9. Representative loss curve for the bulk sample in the Sm- $C^*$  phase. Solid line is a fit to Eq. (2) with the conductivity term (see text). The data shows the presence of only one relaxation mode.

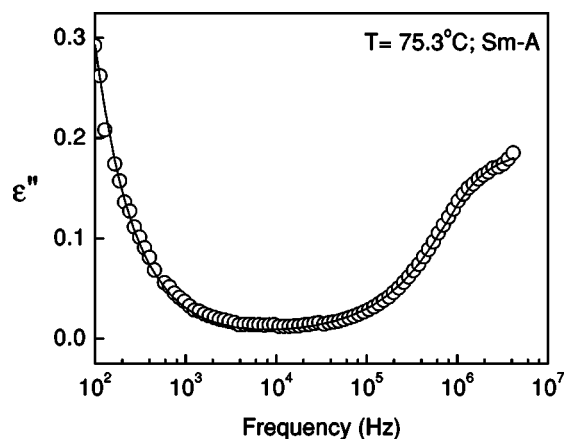


FIG. 10. Representative loss curve for the Anopore sample in the Sm-A phase. Solid line is a fit to Eq. (2) with the conductivity term.

feature to be noticed is that in the Sm- $C^*$  phase even the maximum value of  $\epsilon_{\perp}$  is much smaller than the value obtained for the bulk sample. However, the thermal variation is quite similar to that seen for the bulk sample at low frequencies. These two features indicate that presence of the Goldstone mode, which is partially suppressed. In other words, there is a partial unwinding of the helix driven by the narrow pore size. Further, even at 1 MHz, the behavior is qualitatively similar to the low frequency ones, pointing to the fact, as we shall see later, that the relaxation frequency of the Goldstone has shifted to higher values compared to that for the bulk sample. Figures 8–11 show representative dielectric spectra in the bulk and confined geometries in the Sm-A and Sm- $C^*$  phases. In each case, only one dielectric loss peak is seen and a conductivity-dominated process exists at lower frequencies. Notice that in the Sm- $C^*$  profiles of the bulk sample the dielectric loss peak has a substantially larger strength and occurs at a lower frequency than the ones in the Sm-A phase. In contrast for the Anopore sample, although the strength is slightly larger than that in the Sm-A, the frequencies are not very different. To determine the relaxation

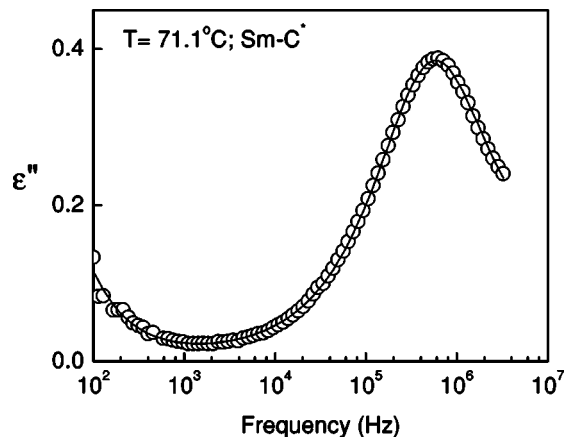


FIG. 11. Representative loss curve for the Anopore sample in the Sm- $C^*$  phase. Solid line is a fit to Eq. (2) with the conductivity term.

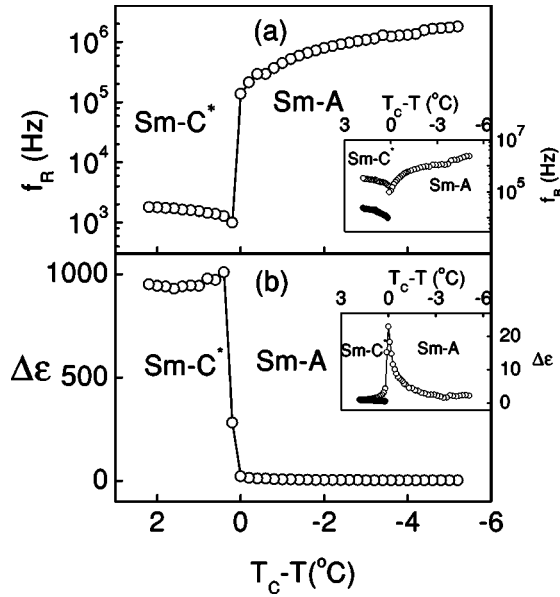


FIG. 12. Dependence of the relaxation frequency ( $f_R$ ) [Fig. 12(a)] and the dielectric strength ( $\Delta\epsilon$ ) [Fig. 12(b)] on reduced temperature  $T_c - T$  (the  $T_c$  being the transition temperature) for the bulk sample across Sm-A–Sm-C\* transition. Due to the dominating influence of the Goldstone mode, the soft mode was not seen in the Sm-C\* phase. Inset shows the thermal variation of  $f_R$  [Fig. 12(a)] and  $\Delta\epsilon$  [Fig. 12(b)] on application of a dc bias voltage ( $0.5 \text{ V}/\mu\text{m}$ ). While the open circles represent data for the soft mode, the filled circles are for the Goldstone mode.

parameters, data collected outside the transition region were analyzed using a Havriliak-Negami function [19]

$$\epsilon^*(f) = \epsilon_\infty + \frac{\Delta\epsilon}{\left[1 + \left(\frac{if}{f_R}\right)^\alpha\right]^\beta}. \quad (2)$$

Here  $f$  is the measuring frequency,  $\epsilon_\infty$  is the sum of the dielectric strengths of all the high frequency modes other than the one under consideration.  $\Delta\epsilon$  is the difference between low and high frequency dielectric constants and is a measure of the dielectric strength of the mode of interest,  $f_R$  is the characteristic relaxation frequency. The parameters  $a$  and  $b$  describe the width and asymmetric broadening of the relaxation curve. To account for the dc conductivity ( $\sigma$ ) contribution to the imaginary part of the dielectric constant, the term  $-i(\sigma/2\pi\epsilon_0 f)$  was added to the right hand side of Eq. (2); here  $\epsilon_0$  is the permittivity of free space. The increase in  $\epsilon''$  in the MHz region (clearly visible in the Sm-A profile for the Anopore sample) was due to the sheet resistance of ITO; a fitting procedure was used to account for it. The best fit of the data to Eq. (2) in addition to a conductivity-dependent term are shown in Figs. 8–11. Through exhaustive work on bulk samples exhibiting Sm-A–Sm-C\* transition, it is now well established that the collective relaxation in these systems can be analyzed in terms of the fluctuations of the two-component tilt order parameter [20]. The amplitude part of the tilt gives rise to the soft mode (SM), which softens on approaching the transition from either of the phases. The

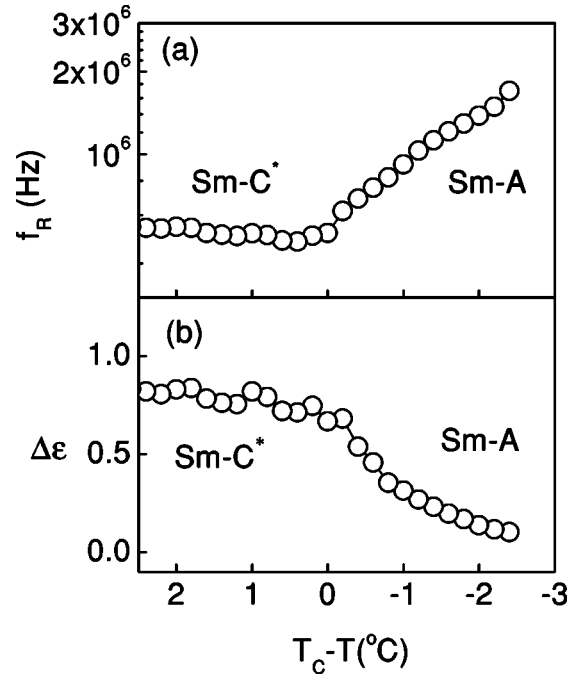


FIG. 13. Plot of  $f_R$  [Fig. 13(a)] and  $\Delta\epsilon$  [Fig. 13(b)] versus  $T_c - T$  for the Anopore sample across the Sm-A–Sm-C\* transition.

azimuthal angle part is responsible for the Goldstone mode (GM), which is active only in the Sm-C\* phase. The GM has a much larger strength and occurs at a lower frequency in comparison with the SM. With this background let us first look at the temperature dependence of  $f_R$  and  $\Delta\epsilon$  for the bulk sample [Figs. 12(a) and 12(b), respectively]. The observed decrease in  $f_R$  and the concomitant increase in  $\Delta\epsilon$ , as the transition is approached from the Sm-A phase, is a feature characteristic of the soft mode. At the transition, the GM appears and due to its overwhelming dielectric strength the soft mode is hardly observed in the Sm-C\* phase. However, application of a dc bias field ( $\sim 0.5 \text{ V}/\mu\text{m}$ ) suppresses the Goldstone mode sufficiently enabling the SM to be seen [see insets of Figs. 12(a) and 12(b)] and also brings out the Curie-Weiss nature of the SM behavior. Notice that the application of dc field increases the relaxation frequency of the GM (by about an order of magnitude) caused by the unwinding of the helix. Figures 13(a) and 13(b) show the data obtained for the Anopore sample. The behavior in the Sm-A phase is identifiable with the one observed for the bulk sample, namely that the relaxation frequency decreases as the transition is approached, while the dielectric strength increases. The magnitude of the relaxation frequency is, however, different. For example, at  $T_c + 1^\circ\text{C}$ , the  $f_R$  value for the Anopore sample is about 2.5 times higher than that for the bulk. The rate at which  $f_R$  decreases on approaching  $T_c$  is also more for the Anopore ( $374 \text{ kHz}/^\circ\text{C}$ ) than for the bulk ( $295 \text{ kHz}/^\circ\text{C}$ ). It is interesting to see that the rate for the bulk sample with bias field ( $363 \text{ kHz}/^\circ\text{C}$ ) is comparable to that of the Anopore sample. In the Sm-C\* phase only one mode is observed, whose relaxation frequency lies in the range of 600 kHz. Although one may like to ascribe such a high frequency relaxation with the soft mode, the temperature-independent

nature of  $f_R$  and the associated  $\Delta\epsilon$  precludes such an interpretation. In fact, the trend seen suggests the behavior of the Goldstone mode. However, it should be noted that these  $f_R$  values are about 400 times larger than the GM of the bulk sample. But as noted earlier, in the presence of a bias field the value of GM increases by about an order of magnitude for the bulk sample. Thus it is tempting to associate the relaxation mode seen in the Sm-C\* phase to that of the GM mode, but with a substantially unwound helix. It may be recalled that Rozanski *et al.* [11] reported a similar (factor of  $\sim 20$ ) increase in the GM relaxation frequency when the material is confined in Synpore membranes having a pore size of 850 nm. Thus, it is possible that in the present case, as was true with the Synpore measurements, that the pitch of the helix being comparable to the pore diameter, gets unwound, at least partially due to the interaction of the liquid crystalline molecules with the walls of the confining membrane. Finally, it must be remarked that with the application of a

bias field we did not find any significant influence on either the magnitude or the thermal behavior of the sample confined in the Anopore membrane. In summary, we have reported on the comparative behavior of a compound exhibiting a first-order smectic A–smectic-C\* transition in bulk as well as in confined geometry. Upon confinement, we find that there is a significant change in the temperature dependence of the layer spacing, and that the relaxation frequency of both the soft mode and Goldstone mode increase, the latter being as much as by 400 times.

#### ACKNOWLEDGMENTS

We are grateful to Professor S. Chandrasekhar for many useful discussions. A research grant from the U.S. Office of Naval Research (ONR Grant No. N00014-97-1-0904) is gratefully acknowledged.

- 
- [1] For an excellent collection of review articles in this field, see *Liquid Crystals in Complex Geometries*, edited by G. P. Crawford and S. Zumer (Taylor & Francis, London, 1996).
- [2] M. Kuzma, and M.M. Labes, *Mol. Cryst. Liq. Cryst.* **100**, 103 (1983).
- [3] G.P. Crawford, R. Stannarius, and J.W. Doane, *Phys. Rev. A* **44**, 2558 (1991).
- [4] G.S. Iannacchione and D. Finotello, *Phys. Rev. Lett.* **69**, 2094 (1992).
- [5] M.D. Dadmun and M. Muthukumar, *J. Chem. Phys.* **98**, 4850 (1993).
- [6] G.P. Sinha and F.M. Aliev, *Phys. Rev. E* **58**, 2001 (1998).
- [7] G.S. Iannacchione, J.T. Mang, S. Kumar, and D. Finotello, *Phys. Rev. Lett.* **73**, 2708 (1994).
- [8] T. Bellini, N.A. Clark, and D.W. Schaefer, *Phys. Rev. Lett.* **74**, 2740 (1995).
- [9] F.M. Aliev, in *Liquid Crystals in Complex Geometries*, edited by G.P. Crawford and S. Zumer (Taylor & Francis, London, 1996), p. 345.
- [10] M. Skarabot, S. Kralj, R. Blinc, and I. Musevic, *Liq. Cryst.* **26**, 723 (1999).
- [11] S.A. Rozanski, R. Strannarius, F. Krenes, and S. Diele, *Liq. Cryst.* **28**, 1071 (2001).
- [12] J. Werner, K. Otto, D. Enke, G. Pelzl, F. Janowski, and H. Kresse, *Liq. Cryst.* **27**, 1295 (2000).
- [13] K.L. Sandhya, Geetha G. Nair, S. Krishna Prasad, and Anjuli Khandelwal, *Liq. Cryst.* **28**, 1847 (2001).
- [14] Ch. Bahr and G. Heppke, *Mol. Cryst. Liq. Cryst.* **148**, 29 (1987).
- [15] Geetha G. Nair, S. Krishna Prasad, R. Shashidhar, B. R. Ratna, Ch. Bahr, and G. Heppke, *Abstracts of the 13th International Liquid Crystal Conference*, PHA-24, Vancouver, Canada, 1990 (unpublished).
- [16] H.Y. Liu, C.C. Huang, Ch. Bahr, and G. Heppke, *Phys. Rev. Lett.* **61**, 345 (1998).
- [17] C.C. Huang and J.M. Viner, *Phys. Rev. A* **25**, 3385 (1982).
- [18] The application of an electric field perpendicular to the layer normal direction in the chiral Sm-A phase leads to the appearance of an induced tilt. Thus, the two phases across the transition (which are Sm-A and Sm-C\* in the absence of the field) become isosymmetric. This situation is similar to that of a system with a gas-liquid transition. Consequently, there can only be a first-order transition between the two phases. In the Sm-A–Sm-C\* case, application of an electric field of certain strength results in a critical point, above which the two phases are indistinguishable and evolve continuously from one to another. For further details, see Ch. Bahr and G. Heppke, *Phys. Rev. A* **41**, 4335 (1990).
- [19] S. Havriliak and S. Negami, *J. Polym. Sci., Part C: Polym. Symp.* **14**, 99 (1966).
- [20] F. Gouda, K. Sarp, and S.T. Lagerwall, *Ferroelectrics* **113**, 169 (1991); S.U. Vallerien, F. Kramer, H. Kapitza, R. Zentel, and W. Frank, *Phys. Lett. A* **138**, 219 (1989); S. Krishna Prasad, S.M. Khened, V.N. Raja, S. Chandrasekhar, and B. Shivakumar, *Ferroelectrics* **138**, 37 (1993).